BIOCHEMICAL PHARMACOLOGY 74 (2007) 623–638

available at www.sciencedirect.com

ScienceDirect

journal homepage: www.elsevier.com/locate/biochempharm

The ω-atracotoxins: Selective blockers of insect M-LVA and HVA calcium channels☆

Youmie Chong[a], *Jessica L. Hayes*[a], *Brianna Sollod*[b], *Suping Wen*[a], *David T. Wilson*[e], *Peter G. Hains*[c], *Wayne C. Hodgson*[d], *Kevin W. Broady*[a], *Glenn F. King*[b,1], *Graham M. Nicholson*[a,*]

[a] *Neurotoxin Research Group, Department of Medical & Molecular Biosciences, University of Technology, Sydney, Broadway, NSW 2007, Australia*
[b] *Department of Molecular, Microbial & Structural Biology, University of Connecticut Health Center, Farmington, CT 06032, USA*
[c] *Save Sight Institute, Sydney Eye Hospital, Macquarie Street, Sydney, NSW 2001, Australia*
[d] *Monash Venom Group, Department of Pharmacology, Monash University, Clayton, Vic. 3800, Australia*
[e] *Institute for Molecular Bioscience, University of Queensland, St. Lucia, Qld 4072, Australia*

ARTICLE INFO

Article history:
Received 18 April 2007
Accepted 22 May 2007

Keywords:
ω-ACTX-Ar1a
ω-ACTX-Hv1a
ω-Atracotoxin
Voltage-gated calcium channel
Insecticide
Atrax robustus

ABSTRACT

The ω-atracotoxins (ω-ACTX) are a family of arthropod-selective peptide neurotoxins from Australian funnel-web spider venoms (Hexathelidae: Atracinae) that are candidates for development as biopesticides. We isolated a 37-residue insect-selective neurotoxin, ω-ACTX-Ar1a, from the venom of the Sydney funnel-web spider *Atrax robustus*, with high homology to several previously characterized members of the ω-ACTX-1 family. The peptide induced potent excitatory symptoms, followed by flaccid paralysis leading to death, in acute toxicity tests in house crickets. Using isolated smooth and skeletal nerve-muscle preparations, the toxin was shown to lack overt vertebrate toxicity at concentrations up to 1 μM. To further characterize the target of the ω-ACTXs, voltage-clamp analysis using the whole-cell patch-clamp technique was undertaken using cockroach dorsal unpaired median neurons. It is shown here for the first time that ω-ACTX-Ar1a, and its homolog ω-ACTX-Hv1a from *Hadronyche versuta*, reversibly block *both* mid–low- (M-LVA) and high-voltage-activated (HVA) insect calcium channel (Ca_v) currents. This block occurred in the absence of alterations in the voltage-dependence of Ca_v channel activation, and was voltage-independent, suggesting that ω-ACTX-1 family toxins are pore blockers rather than gating modifiers. At a concentration of 1 μM ω-ACTX-Ar1a failed to significantly affect global K_v channel currents. However, 1 μM ω-ACTX-Ar1a caused a modest 18% block of insect Na_v channel currents,

☆ The amino acid sequence of ω-ACTX-Ar1a reported in this paper has been deposited in the Swiss-Prot Database under accession code P83580. The DNA sequences of the ω-ACTX-Ar1 family have been deposited in GenBank under accession numbers EF523494, EF523495, EF523497, EF523498, and EF523499.

* *Corresponding author at*: Neurotoxin Research Group, Department of Medical & Molecular Biosciences, University of Technology, Sydney, P.O. Box 123, Broadway, NSW 2007, Australia. Tel.: +61 2 9514 2230; fax: +61 2 9514 8206.
E-mail address: Graham.Nicholson@uts.edu.au (G.M. Nicholson).
[1] Current address: Institute for Molecular Bioscience, University of Queensland, St. Lucia, Qld 4072, Australia.

Abbreviations: ω-ACTX, ω-atracotoxins from Australian funnel-web spiders; BK_{Ca} channel, large conductance calcium-activated potassium channel; Ca_v channel, voltage-gated calcium channel; CNS, central nervous system; DUM, dorsal unpaired median; ESI-Q-ToF, electrospray ionization quadrupole time-of-flight; HEPES, N-2-hydroxyethylpiperazine-N-2-ethanesulfonic acid; HVA, high-voltage-activated; IC_{50}, median inhibitory concentration; ICK, inhibitory cystine-knot; KD_{50}, median knockdown dose; K_v channel, voltage-gated potassium channel; LD_{50}, median lethal dose; M-LVA, mid-low-voltage-activated; MIT, mamba intestinal toxin; Na_v channel, voltage-gated sodium channel; rpHPLC, reverse-phase high-performance liquid chromatography; TAG, terminal abdominal ganglion; TFA, trifluoroacetic acid; TEA, tetraethylammonium; (+)-TC, (+)-tubocurarine; TTX, tetrodotoxin

0006-2952/$ – see front matter
doi:10.1016/j.bcp.2007.05.017

similar to the minor block of Na_v channels reported for other insect Ca_v channel blockers such as ω-agatoxin IVA. These findings validate both M-LVA and HVA Ca_v channels as potential targets for insecticides.

1. Introduction

The evolution of insect resistance to one or more classes of commonly used agrochemicals has now been reported in most major insect crop pests and disease vectors [1,2]. Over the period 1996–1998, pests were estimated to destroy around 18% of the world's food supply, with the major damage being caused by arthropods [3]. In addition, arthropods are vectors for the transmission of many new and re-emerging diseases of significant medical and veterinary importance [4]. This has necessitated the development of new strategies to combat highly resistant herbivorous and hematophagous pest species. New biological approaches include the production of transgenic crops that express insecticidal toxins from the soil bacterium *Bacillus thuringiensis* [5] and the release of insect-specific recombinant baculoviruses that express a variety of insecticidal neurotoxins from animal venoms [6]. Recent studies have investigated the potential of expressing ω-atracotoxins from the venom of Australian funnel-web spiders in plants or as orally active acaricidal agents [7,8].

The ω-atracotoxin-1 (ω-ACTX-1) toxins constitute the first family of insect-specific peptide toxins isolated from the venom of Australian funnel-web spiders (Mygalomorphae: Hexathelidae: Atracinae). These toxins are reported to inhibit insect, but not mammalian, Ca_v channels [9–12]. All family members are 36–37 residues in length, and contain six cysteine residues with a strictly conserved disulfide pattern. The three-dimensional solution structure of ω-ACTX-Hv1a comprises a structurally disordered N-terminus (residues 1–3), a core region rich in β-turns and disulfides (residues 4–21), and a β-hairpin (residues 22–37) that protrudes from the disulfide-rich core [10]. The three disulfide bonds form an inhibitory cystine-knot (ICK) motif that is present in the majority of atracotoxin structures determined to date, and which is common in peptide neurotoxins targeting ion channels [13–15]. Site-directed mutagenesis [11] and synthetic truncates [9] have been used to elucidate the toxin insectophore, the key residues involved in binding to the insect target site, of the prototypic family member ω-ACTX-Hv1a. The primary insectophore residues, Pro^{10}, Asn^{27} and Arg^{35}, form a small contiguous patch of ~200 $Å^2$ on one face of the toxin surface [11,12] (Fig. 1C). Residues Gln^9 and Tyr^{13} appear to be of minor functional importance in orthopterans and dictyopterans, but not dipterans, suggesting that there might be minor species-specific variations in the toxin insectophore (Fig. 1C).

These toxins are lethal over a wide range of arthropod orders including Acarina, Coleoptera, Dictyoptera, Diptera, Hemiptera, Lepidoptera, and Orthoptera [7,8,10,11,16–18]. ω-ACTX-1 toxins cause irreversible spastic paralysis, preceeding flaccid paralysis and death, yet no toxic effects have been reported following testing on vertebrate preparations. In insect preparations, ω-ACTX-Hv1a acts directly on CNS neurons rather than interganglionic axons or the peripheral neuromuscular junction [10,17]. Electrophysiological studies have shown that the phyletic specificity of this family of toxins is believed to be derived from their action on invertebrate, but not vertebrate, voltage-gated calcium (Ca_v) channels [10,12]. In preliminary experiments in unidentified cockroach metathoracic ganglia neurons, ω-ACTX-Hv1a partially blocked Ca_v channels at concentrations up to 1 μM. Competitive binding assays using radioiodinated ω-atracotoxin-Hv1a revealed that the toxin binds to orthopteran channels at nanomolar concentrations [12], whereas it had no effect on whole-cell Ca_v channel currents in a variety of vertebrate-derived neuron preparations at concentrations as high as 1 μM [10]. Moreover, the toxin does not block rat HVA $Ca_v1.2$ (L-type), $Ca_v2.1$ (P/Q-type) or $Ca_v2.2$ (N-type) channels at concentrations up to 10 μM [12]. However, the mode of channel block and the precise insect Ca_v channel subtype targeted by the ω-ACTX-1 toxins remains to be determined, and their potential action on other voltage-gated ion channels has not been investigated in detail.

Recently, ω-ACTX-Hv1a has been trialed as a novel biopesticide for protection of plants from phytophagous pest insects following expression of the toxin transgene in tobacco plants (*Nicotiana tabacum*). Transgenic expression of ω-ACTX-Hv1a effectively protected tobacco plants from the larvae of two recalcitrant agricultural pests, *Helicoverpa armigera* and *Spodoptera littoralis*, with 100% mortality at 48 h [7]. Surprisingly, a recombinant thioredoxin–ω-ACTX-Hv1a fusion protein was lethal to *H. armigera* and *S. littoralis* caterpillars when applied topically [7]. In addition, ω-ACTX-Hv1a is orally active against ticks [8] and mosquitoes (J. Huang, G. King, S. Wikel, unpublished data). These studies indicate that at least some insecticidal peptide toxins have the potential to be developed as orally active biopesticides.

Here we describe the pharmacological characterization of a novel member of the ω-ACTX-1 family that we isolated from the venom of the Sydney funnel-web spider, *Atrax robustus*. This 37-residue peptide, ω-ACTX-Ar1a, shows selective toxicity against house crickets, but it has no affect on vertebrate nerve-muscle preparations. We show that ω-ACTX-Ar1a and ω-ACTX-Hv1a block both M-LVA and HVA Ca_v channels in cockroach neurons, with minor activity against Na_v but not K_v channels. This block did not alter the voltage-dependence of Ca_v channel activation, and it was voltage-independent, suggesting that the ω-ACTX-1 toxins are pore blockers rather than gating modifiers. As far as we are aware, the ω-ACTX-1 toxins are the first peptide toxins demonstrated to selectively block both M-LVA and HVA insect Ca_v channels.

2. Materials and methods

2.1. Toxin purification and peptide sequencing

Venom was collected from female Sydney funnel-web spiders, *A. robustus*, via direct aspiration from the fangs. Venom was

then pooled and fractionated using reverse-phase high performance liquid chromatography (rpHPLC) employing a Vydac analytical column (C18, 4.6 mm × 250 mm, 5 μm) on a Shimadzu HPLC system. Peptide peaks were monitored at an absorbance of 215 nm. Elution of venom peptide components was achieved using a linear gradient of 5–25% acetonitrile/0.1% trifluoroacetic acid (TFA) over 20 min, then 25–50% acetonitrile/0.1% TFA over 20 min at flow rate of 1.0 mL/min. Selected fractions were subjected to acute toxicity bioassays using house crickets to determine insect toxicity (see Section 2.2). The major toxic fraction, ω-ACTX-Ar1a (peak '*f*9' in Fig. 2A) was further purified on an analytical C18 rpHPLC column using a linear gradient of 5–14% acetonitrile/0.1% TFA over 5 min, then 14–16% acetonitrile/0.1% TFA over 20 min, at a flow rate of 1 mL/min (Fig. 2B). Purified toxin was collected, lyophilized, and stored at −20 °C until required. Toxin quantification was performed using a bicinchoninic acid protein assay kit (Pierce, Rockford, IL, USA) using bovine serum albumin as a standard. The molecular mass of the toxin was determined, via electrospray ionization quadrupole time-of-flight (ESI-Q-ToF) mass spectrometry using a Q-ToF2 system (Micromass, Manchester, England) equipped with a nanospray source. Data was manually acquired in the positive mode using borosilicate capillaries with a source temperature of 80 °C. Samples were dissolved in 5 μL 50% acetonitrile and 0.5% formic acid. A potential of 850 V was applied to the nanoflow tip. Raw data were processed using the MaxEnt algorithm included in the MassLynx program. In preparation for amino acid sequencing using Edman degradation, the toxin was reduced and cysteine residues were pyridylethylated with 4-vinylpyridine and purified using rpHPLC as described previously [10]. The entire peptide sequence was then obtained from a single sequencing run on an Applied Biosystems/Perkin-Elmer Procise 492 cLC protein sequencer.

ω-ACTX-Hv1a was obtained by overproduction of a glutathione *S*-transferase (GST)-toxin fusion protein in *E. coli* cells as described previously [11]. Briefly, the recombinant fusion protein was purified from the soluble cell fraction using affinity chromatography on glutathione-sepharose, then the toxin was released by on-column thrombin cleavage and purified to >98% homogeneity using C18 rpHPLC. The identity of the toxin was confirmed using ESI mass spectrometry [11].

2.2. Invertebrate toxicity assays

For quantitative analysis of insecticidal activity, purified toxin was dissolved in insect saline of the following composition (in mM): NaCl 200, KCl 3.1, $CaCl_2$ 5.4, $MgCl_2$ 4, $NaHCO_3$ 2, Na_2HPO_4, 0.1% (w/v) bovine serum albumin, pH 7.4. House crickets (*Acheta domestica* Linnaeus, 3rd–4th instar nymphs, sex not determined) of mass 50–100 mg were then injected with toxin at concentrations of 5–2000 pmol/g; injection volumes never exceeded 5 μL. An Arnold micro-applicator (Burkhard Scientific Supply, Rickmansworth, England) was used to make lateroventral thoracic injections between legs 2 and 3 using a 29-gauge needle. Ten crickets were injected at each concentration; a group of 10 control crickets each received an injection of insect saline only. Insects were monitored for 72 h following injection. Percentage knockdown and lethality were determined at 12, 24, 48 and 72 h post-injection. Knockdown was defined as the inability to maintain an upright posture, with intermittent or continuous twitches of appendages. Median knockdown (KD_{50}) and median lethal (LD_{50}) doses were then determined from log dose–response curves (see Section 2.6).

2.3. Isolated vertebrate bioassays

Vertebrate toxicity was investigated using isolated chick biventer cervicis nerve-muscle preparations as described previously [19]. Briefly, muscles were removed from male Australorp chicks (1–4 days old), mounted in 8-mL organ baths under 1 g resting tension, then bathed in Krebs–Henseleit solution containing (in mM): NaCl 118.4, KCl 4.7, $CaCl_2$ 2.5, $MgSO_4$ 1.2, KH_2PO_4 1.2, $NaHCO_3$ 25.0, D-glucose 11.1, pH 7.4. The muscle was maintained at 34 °C and constantly carbogenated with 95% O_2 and 5% CO_2. Isometric twitch contractions were elicited by indirect stimulation of the motor nerve (supramaximal voltage, 0.05–0.2 ms, 0.1 Hz), via ring electrodes. Responses to exogenous acetylcholine (1 mM, 30 s) and KCl (40 mM, 30 s) were obtained prior to the addition of venom and at the conclusion of the experiment. For preparation of vas deferens tissue, Sprague Dawley rats (250–350 g) were killed by 80% CO_2 and decapitation. The vas deferens were isolated and bisected to obtain prostatic segments and mounted on electrodes in 5-mL organ baths at 32 °C under 0.75 g resting tension. Indirect twitches were evoked by electrical stimulation of the motor nerve (supramaximal voltage, 0.3 ms, 0.2 Hz). Preparations were allowed to equilibrate for at least 30 min with continuous stimulation before the addition of toxin or venom. All animal experimentation was approved by the Animal Care & Ethics Committees of the University of Technology, Sydney or Monash University. Responses were recorded for 30 min following the introduction of purified toxin to the organ bath at concentrations up to 1 μM. Contractions of muscles were recorded using a MacLab or PowerLab data acquisition system (AD Instruments, Castle Hill, NSW, Australia).

2.4. DNA sequence of the complete ω-ACTX-Ar1a transcript

2.4.1. Preparation of cDNA

Pairs of venom glands were dissected from one male and one female *A. robustus* spider, then poly-A+ mRNA was prepared from each pair of glands using a QuickPrep Micro mRNA Purification Kit (Amersham Pharmacia Biotech). cDNA libraries were constructed from the mRNA using a Marathon cDNA Amplification Kit (Clontech). From the adapted mRNA template, single-stranded cDNA was constructed using Superscript III reverse transcriptase (Life Technologies Inc.) and a poly-(dT) anchor primer. Second strand synthesis was carried out as per kit specifications using DNA polymerase I. The resulting double-stranded cDNA products were purified using a concert rapid PCR purification kit (GIBCO) then ligated to a Marathon cDNA amplification adaptor (Clontech) to provide a handle for rapid amplification of cDNA ends (RACE; [20]). Samples were ligated overnight at 16 °C, precipitated using glycogen–acetate–ethanol, then washed with 80% ethanol and dried for 10 min prior to resuspension in 200 μL of Tris-EDTA buffer.

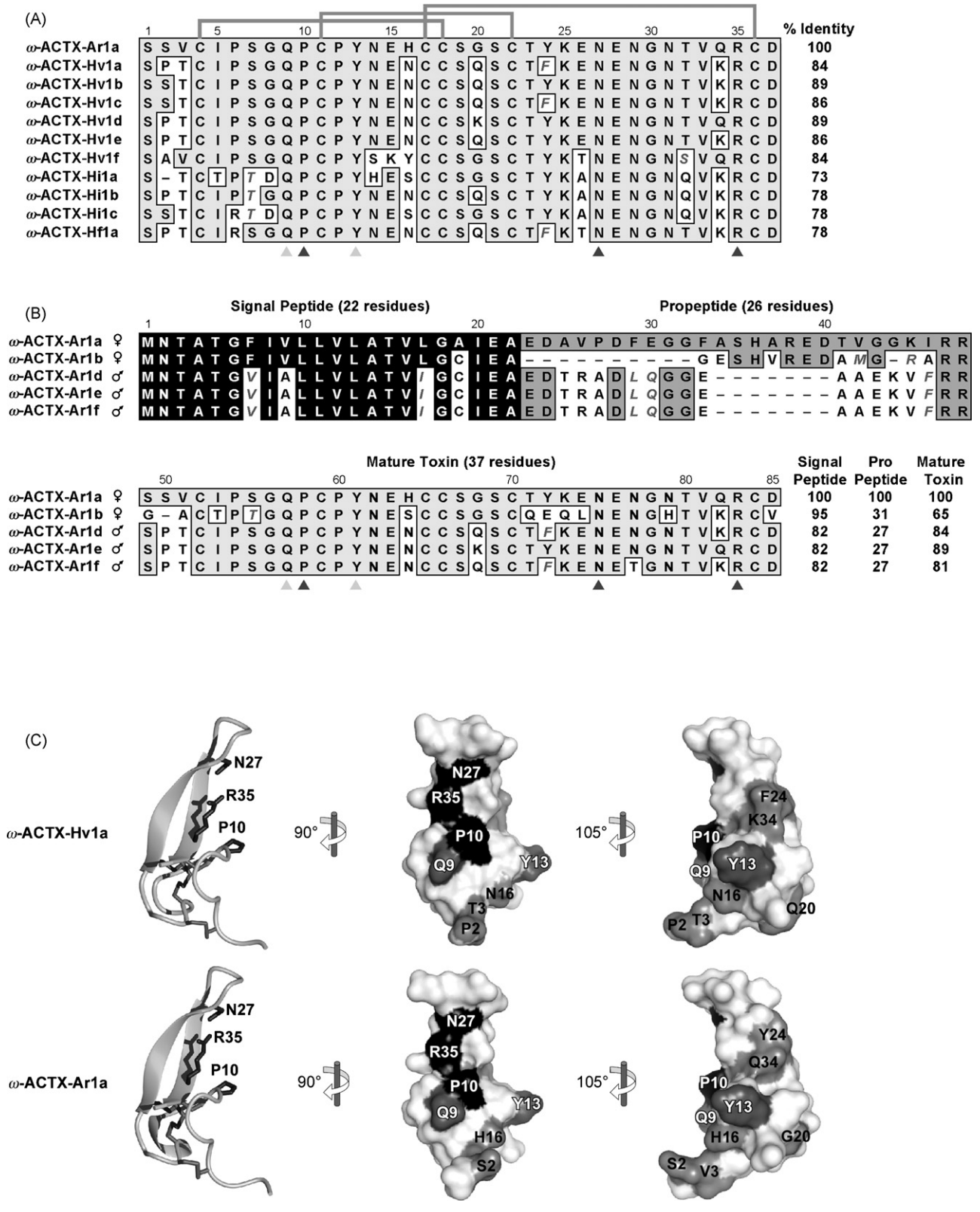

Fig. 1 – (A) Alignment of the primary structure of ω-ACTX-Ar1a with known members of the ω-ACTX-1 family, isolated from *Hadronyche versuta* (Hv), *Hadronyche infensa* (Hi) and *Hadronyche formidabilis* (Hf). Identities are boxed in gray, conservative substitutions are in grey italic text, and the disulfide bonding pattern of ω-ATCX-Hv1a is shown by the gray lines, connecting Cys residues, above the sequences. The major insectophore, identified for ω-ACTX-Hv1a [11], is shown by the black arrowheads beneath the sequences, while additional residues forming a minor insectophore in orthopterans and dictyopterans, but not dipterans, are in shown as gray arrowheads [12]. Note that these residues are conserved in the sequence of ω-ACTX-Ar1a. The column on the right indicates the % identity relative to ω-ACTX-Ar1a. (B) The primary

2.4.2. RACE analyses

The leader sequence of the mRNA transcript encoding ω-ACTX-Ar1a was obtained from 5′-RACE analysis [21], which employed a redundant 3′-primer based on the known amino acid sequence of the mature ω-ACTX-Hv1a toxin (5′-RTTNCCRTTYTCRTTYTCYTCRAA, where Y = T + C and N = A + G + T + C) and a 5′-universal adaptor primer (EchoAP1). A 3′-RACE primer based on the leader sequence obtained from 5′-RACE analysis was then used in combination with a 5′-universal adaptor oligo-d(T) primer (Clontech) to generate full-length sequences for ω-ACTX-Ar1a and paralogs. All primers not included in kits were constructed by PROLIGO Ltd.

2.4.3. PCR amplification and sequencing

PCR reactions were run on a thermal cycler using the following protocol: 95 °C for 5 min (1 cycle); 35 cycles of 95 °C for 30 s, 55 °C for 60 s, and 72 °C for 90 s; 72 °C for 10 min (1 cycle). Amplified cDNA products were electrophoresed on a 1.5% agarose gel and stained with ethidium bromide for size verification. Verified PCR products were extracted using a GIBCO gel purification kit, precipitated using Pellet Paint Co-Precipitant kit (Novagen), then phosphorylated in preparation for cloning. Samples were ligated into the pSMART vector (Lucigen) then transformed into *E. cloni® competent* cells using the CloneSmart Blunt Cloning kit (Lucigen). Successfully transformed clones were cultured for 1 h in Terrific Broth containing 50 μg/mL ampicillin, then plated to allow for overnight growth. Samples containing the expected insert size of ~500 bp (as verified using PCR and gel electrophoresis) were submitted for DNA sequencing.

2.5. Electrophysiological studies

Dorsal unpaired median (DUM) neurons, from the terminal abdominal ganglion (TAG) of the nerve cord of the male adult American cockroach *Periplaneta americana*, were isolated using methods modified from Grolleau and Lapied [22] and Wicher and Penzlin [23]. Median sections of the TAG, known to contain the highest number of DUM neurons [24], were dissected and individual DUM neurons were dissociated using a combination of mechanical and enzymatic separation techniques. The TAG was carefully dissected and placed in sterile Ca^{2+}- and Mg^{2+}-free insect saline of the following composition (in mM): 200 NaCl, 3.1 KCl, 10 N-2-hydroxyethyl-piperazine-N-2-ethanesulfonic acid (HEPES) and 60 sucrose. The ganglia were then desheathed and incubated at 37 °C for 15 min in Ca^{2+}- and Mg^{2+}-free insect saline containing collagenase (1 mg/mL) and hyaluronidase (1 mg/mL). The ganglia were then centrifuged and rinsed three times in normal insect saline of the following composition (in mM): 200 NaCl, 3.1 KCl, 5 $CaCl_2$, 4 $MgCl_2$, 10 HEPES, 50 sucrose, supplemented with bovine calf serum (5%, v/v), penicillin (50 IU/mL) and streptomycin (50 μg/mL) (Trace Biosciences, Noble Park, Australia). DUM neurons were then mechanically isolated from exogenous tissue by trituration, carefully passing the ganglia in and out of a sterile Pasteur pipette. The resulting suspension was then distributed into eight wells of a 24-well cluster plate (Limbro, Ohio, USA). Each well contained a 12-mm diameter glass coverslip (Lomb Scientific, Taren Point, NSW) that had been previously coated with 1 mg/ml concanavalin-A (Type VI) (Sigma Chemicals, Castle Hill,

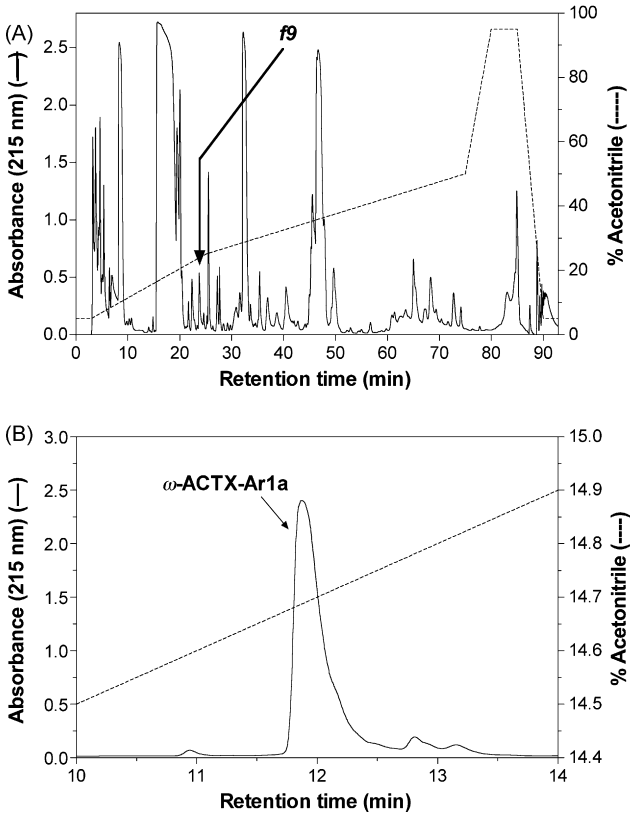

Fig. 2 – Reverse-phase HPLC chromatogram of female *A. robustus* venom. (A) Screening of venom fractions revealed that the peak labeled *f*9 induced toxicity when injected into house crickets. (B) Further rpHPLC purification of *f*9 using a shallow acetonitrile gradient yielded three peaks, the largest of which (ω-ACTX-Ar1a) was found to be responsible for the insect toxicity of fraction *f*9.

structures of the ω-ACTX-Ar1a prepropeptide and four paralogs thereof derived from analysis of a cDNA library prepared from female and male *Atrax robustus* venom glands. The propeptide cleavage site was readily discerned from the known ω-ACTX-Ar1a mature toxin sequence, shown in (A), while the consensus signal peptide cleavage site was predicted by the SignalP program [29]. (C) Structure of ω-ACTX-Hv1a and ω-ACTX-Ar1a. The upper panels show the NMR structure of ω-ACTX-Hv1a (PDB file 1AXH) while lower panels show the structure of ω-ACTX-Ar1a modeled on the known structure of ω-ACTX-Hv1a using the automated protein homology-modeling server SWISS-MODEL [44,45]. In each panel, the left-hand view shows a schematic of the 3D structure highlighting the location of β-strands (gray arrows), the side chains of residues forming the major insectophore (Pro^{10}, Asn^{27}, Arg^{35}), and the disulfide bridges (gray tubes). The two views on the right show surface representations indicating the location of the major (black) and minor (dark gray) insectophore residues, as well as residues that differ between the two toxin sequences at positions 2, 3, 16, 20, 24, and 34 (gray).

NSW) or Cell-Tak (BD Biosciences, Australia). Isolated cells were allowed to attach to the coverslips overnight in an incubator (10% CO_2, 90% O_2, 100% relative humidity, 28 °C). DUM neurons were maintained at 28 °C for 12–24 h before electrophysiological experiments were carried out.

Standard whole cell voltage-clamp recordings of calcium (I_{Ba}), sodium (I_{Na}), and potassium (I_K) channel currents were made from DUM neurons. Due to the report of I_{Ca} rundown with calcium as a charge carrier [22], as well as reports of greater success when barium was used as the charge carrier [23], $BaCl_2$ replaced $CaCl_2$ in all experiments. Recordings of I_{Ba} were made with fire-polished borosilicate pipettes of ~2 MΩ resistance when filled with an internal pipette solution containing (in mM): 10 sodium acetate, 110 CsCl, 50 tetraethylammonium (TEA)-Br, 2 ATP-Na_2, 0.5 $CaCl_2$, 10 EGTA and 10 HEPES, pH adjusted to 7.25–7.35 with CsOH. For recording I_{Na} the internal pipette solution contained (in mM): 135 CsF, 1 $MgCl_2$, 20 NaCl, 10 HEPES and 5 EGTA, with the pH adjusted to 7.25–7.35 with CsOH. For recording macroscopic I_K pipettes contained (in mM): 135 KCl, 25 KF, 9 NaCl, 3 ATP-Mg_2, 1 $MgCl_2$, 0.1 $CaCl_2$, 1 EGTA and 10 HEPES, pH adjusted to 7.25 with NaOH. The external solution for recording I_{Ba} contained (in mM): 160 sodium acetate, 30 TEA-Br, 3 $BaCl_2$ and 10 HEPES, with the pH adjusted to 7.4 using TEA-OH. The external solution for recording I_{Na} contained (in mM): 130 NaCl, 5 CsCl, 1.8 $CaCl_2$, 20 TEA-Cl, 1 4-aminopyridine, 10 HEPES, 0.01 (±)-verapamil, 0.1 $NiCl_2$ and 0.1 $CdCl_2$ with the pH adjusted to 7.4 using NaOH. The external solution for recording I_K contained (in mM): 130 NaCl, 20 KCl, 5 $CaCl_2$, 1.5 $MgCl_2$, 1 $CdCl_2$, 10 HEPES, pH adjusted to 7.4 using NaOH. The osmolarity of both internal and external solutions was determined with a cryoscopic osmometer (Gonotec Osmomat 030, Berlin, Germany) and adjusted to 420–430 mOsm/L with sucrose to reduce osmotic stress. The external solution was applied to the perfusion chamber, via a pressured perfusion system (Automate Scientific, San Francisco, CA, USA) at a flow rate of 0.5–1 mL/min. Data were recorded at room temperature (20–23 °C) which did not fluctuate more than 1 °C during the course of an experiment. Inverted voltage-clamp command pulses were applied to the bath through a Ag/AgCl pellet/3 M KCl-agar bridge. The liquid junction potential between internal and external solutions was determined using the program JPCalc [25], and all data were compensated for this value. The experiments used in this study were rejected if there were large leak currents or currents showed signs of poor space clamping such as an abrupt activation of currents upon relatively small depolarizing pulses. Stimulation and recording were both controlled by the pClamp v9.0 data acquisition system (Molecular Devices, CA, USA). Data were filtered at 5 kHz (four-pole lowpass Bessel filter) and the digital sampling rates were 20 kHz. Leakage and capacitive currents were digitally subtracted with *P-P*/4 procedures [26] and series resistance compensation was set at >80% for all cells. Neurons were voltage clamped at −90 mV, and currents were evoked by stepping the membrane potential from −90 to +40 mV (for I_{Ba}), −80 to +70 mV (for I_{Na}), and −80 to +40 mV (for I_K). Tetrodotoxin (TTX) 500 nM, a known insect Na_v channel blocker [27], or Cd^{2+} 500 μM, a known insect Ca_v channel blocker [23], were used to abolish inward I_{Na} or I_{Ba} currents respectively, and confirmed the currents recorded were carried through these channels.

2.6. Data analysis

Data analyses were performed off-line following completion of the experiment. Mathematical curve fitting was accomplished using GraphPad Prism version 4.00 for Macintosh (GraphPad Software, San Diego, CA, USA). All curve-fitting routines were performed using non-linear regression analysis employing a least squares method. All data shown represent the mean ± S.E. Dose–response curves to determine LD_{50}, KD_{50}, and IC_{50} values were fitted using the following form of the logistic equation:

$$y = \frac{1}{1 + ([x]/\mathrm{Dose}_{50})^{n_H}} \quad (1)$$

where x is the toxin dose, n_H the Hill coefficient (slope parameter), and Dose_{50} is the median inhibitory dose causing lethality, knockdown or block of membrane currents, respectively.

On-rates were determined by fitting timecourse data with the following single exponential decay function:

$$y = A\,e^{-kx} + C \quad (2)$$

where x is the time, A the normalized current value (usually 1.0) before application of toxin, and C is the final normalized current value following block by the toxin. The on-rate (τ_{on}) was determined from the inverse of the rate constant k.

Off-rates were determined by fitting timecourse data with the following single exponential association function:

$$y = C + A(1 - e^{-kx}) \quad (3)$$

where x is the time, A the normalized current value after washout of the toxin (usually 1.0 if complete washout occurred), and C is the normalized current value prior to washout of the toxin. The off-rate (τ_{off}) was determined from the inverse of the rate constant k.

Current–voltage (I/V) curves were fitted using the following equation:

$$I = g_{max}\left(1 - \left(\frac{1}{1 + \exp[(V - V_{1/2})/s]}\right)\right)(V - V_{rev}) \quad (4)$$

where I is the amplitude of the peak current (either I_{Ba}, I_{Na} or I_K) at a given test potential V, g_{max} the maximal conductance, $V_{1/2}$ the voltage at half-maximal activation, s the slope factor, and V_{rev} is the apparent reversal potential.

3. Results

3.1. Isolation of a novel insecticidal toxin

Fig. 2 shows a typical rpHPLC fractionation of crude venom from female *A. robustus*. 45 fractions were individually assayed for insect and vertebrate toxicity. The fraction containing the toxin eluted at 33% acetonitrile/0.1% TFA (peak *f*9, Fig. 2A). This

fraction failed to alter neurotransmission on chick biventer cervicis nerve-muscle preparation at a dose of 10 μg/mL (data not shown). However, injection of 10 μg/g *f*9 into house crickets caused both excitatory and depressant toxic effects. This fraction was pooled and lyophilized, and further purification using C18 rpHPLC with a shallow acetonitrile gradient yielded three distinct components (Fig. 2B). The major peak, labeled 'ω-ACTX-Ar1a', was subsequently shown to be the active component in invertebrate toxicity assays (see Section 3.3). ESI-Q-ToF mass spectrometry revealed that the molecular mass of the peptide was 4002.8 ± 1.0 Da.

3.2. *Toxicity bioassays*

Acute insect toxicity testing in house crickets (*Atrax domesticus*) resulted in signs of toxicity within 15 min following injection of ω-ACTX-Ar1a at doses >100 pmol/g. These signs were initially characterized by increased abdominal contractions, occasional spasms of limbs and antennae, and decreased feeding activity. Signs steadily progressed to high frequency twitching of limbs, antennae and mandibles, with a concurrent loss of coordinated locomotion and righting reflexes. At this stage, crickets were characterized as having reached the 'knockdown' (KD) end-point. Progressive spastic paralysis was then followed by a period of flaccid paralysis, leading to death. The excitatory spastic response followed by a depressed stage prior to death has previously been shown to be the typical phenotype following injection of members of the ω-ACTX-1 family into a wide range of insects [9,10,16,17,28]. Following injection of ω-ACTX-Ar1a, no affected crickets recovered from the toxic effects over a time-course of 72 h. ω-ACTX-Ar1a was found to have an LD_{50} of 236 ± 28 pmol/g, and a KD_{50} of 147 ± 16 pmol/g (Fig. 3A), determined at a 48 h end-point ($n = 4$). However, if 72 h was taken as the endpoint, a marked decrease in the values for both the LD_{50} and the KD_{50} was noted, to 143 ± 10 pmol/g ($n = 4$) and 124 ± 12 pmol/g ($n = 4$), respectively (Fig. 3B).

Following purification of ω-ACTX-Ar1a from crude *f*9, confirmatory testing for lack of vertebrate toxicity was carried out using smooth and skeletal nerve-muscle preparations. At a concentration of 1 μM (equivalent to 4 μg/mL), no effects were seen on the twitch or resting skeletal muscle tension or on the responses to cholinergic agonists, and there was no evidence of any muscle fasciculation (Fig. 3C). The lack of effects on neuromuscular transmission were also confirmed using the electrically stimulated rat vas deferens smooth muscle preparation (Fig. 3C). The lack of any overt toxic action on the wide range of vertebrate receptors and ion channels present in these preparations provide strong evidence for the insect-selective actions of ω-ACTX-Ar1a.

3.3. *Determination of amino acid sequence*

The purified peptide was reduced and the cysteines pyridylethylated in preparation for automated N-terminal amino acid sequencing and to assist in determining the number of cysteine residues. The phenylthiohydantoin-Cys residues with a pyridylethylated sidechain are stable during automated N-terminal amino acid sequencing and therefore allows positive identification of Cys residues. Mass spectral analysis

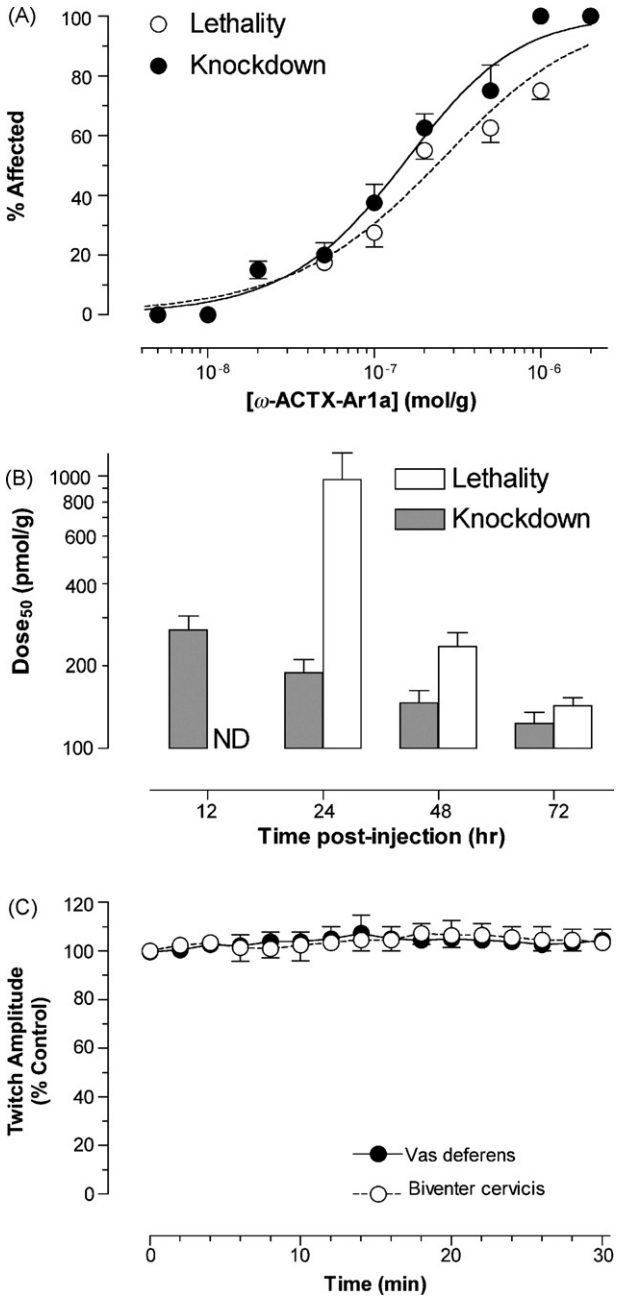

Fig. 3 – Acute toxicity of ω-ACTX-Ar1a in house crickets (*Acheta domesticus*). (A) Log-dose–response curve for death (open circles) and knockdown (closed circles) of crickets by ω-ACTX-Ar1a at 48 h post-injection. Data was fitted with Eq. (1) (see Section 2) to yield a KD_{50} value of 147 ± 16 pmol/g and LD_{50} value of 236 ± 28 pmol/g ($n = 4$). (B) KD_{50} (grey columns) and LD_{50} (open columns) of ω-ACTX-Ar1a at increasing times following intrathoracic injection ($n = 4$). ND indicates that the LD_{50} could not be determined at 12 h post-injection. (C) Timecourse of twitch amplitude in isolated rat vas deferens and chick biventer cervicis nerve-muscle preparations in the presence of 600 nM and 1 μM ω-ACTX-Ar1a, respectively ($n = 2–3$).

of the pyridylethylated toxin revealed a molecular weight of 4640.97 ± 0.41 Da, indicating the presence of six cysteine residues within the primary sequence. The amino acid sequence of the toxin (Fig. 1A), obtained in a single sequencing run without the need to resort to proteolytic digestion, revealed that it contains 37-residues, including six cysteines. The predicted monoisotopic mass of 4002.59 Da for the fully oxidized peptide, in which the six cysteine residues form three disulfide bonds, is consistent with the mass spectral analysis.

A BlastP search of the Swiss-Prot/TrEMBL database revealed that the toxin displayed significant homology with known members of the ω-ACTX-1 family (Fig. 1). The highest homology of 89% was seen with both ω-ACTX-Hv1b and -Hv1d. Members of this toxin family are insect-selective Ca_v channel blockers, and they have been isolated previously from other species of Australian funnel-web spiders belonging to the *Hadronyche* genus, namely *Hadronyche versuta*, *Hadronyche infensa*, and *Hadronyche formidabilis* [9]. Importantly, the number and spacing of cysteine residues, as well as the primary insectophore residues (Pro^{10}, Asn^{27}, Arg^{35}) that are critical for binding to insect Ca_v channels [11,12], are conserved in the newly isolated toxin. The minor insectophore residues Gln^{9} and Tyr^{13}, which are important for activity in cockroaches and crickets (but not flies) [12], are also present. However, the minor insectophore residue Asn^{16} in ω-ACTX-Hv1a, which is known to be important for activity in crickets [12], was substituted by His^{16} in the new toxin. Based on these sequence similarities with ω-ACTX-Hv1a, we have named the new peptide ω-ACTX-Ar1a, and deposited the sequence in the SwissProt (accession no. P83580). ω-ACTX-Ar1a is the first insecticidal toxin isolated from the venom of *A. robustus*.

3.4. Elucidation of ω-ACTX-Ar1a precursor structure

Sequencing of RACE-derived clones revealed the full-length sequences of mRNA transcripts encoding ω-ACTX-Ar1a and four paralogous toxins expressed in the venom gland of either male or female *A. robustus* spiders. The DNA sequences have been deposited in GenBank under accession numbers EF523494, EF523495, EF523497, EF523498, and EF523499. The derived amino acid sequences (Fig. 1B) reveal that the mature toxins are obtained from processing of a larger prepropeptide precursor. The propeptide cleavage site was readily discerned from the known ω-ACTX-Ar1a mature toxin sequence (see Section 3.3), while a consensus signal peptide cleavage site was predicted by the SignalP program ([29]; program available on the web at http://www.cbs.dtu.dk/services/SignalP).

The propeptide architecture is similar to that described for other atracotoxins [12,30–32] and comprises a 22-residue N-terminal signal sequence followed by a propeptide sequence of 15–26 residues that precedes a single downstream copy of the mature toxin sequence (36–37 residues). No transcripts were identified that encoded multiple mature toxin sequences. The mature toxin sequence predicted from the ω-ACTX-Hv1a transcript exactly matches the sequence obtained from Edman degradation of the purified mature toxin.

The signal peptide sequence is strongly conserved among this toxin family, with only four sites out of 22 showing any variation in the five paralogs. This is consistent with the hypothesis that the signal sequence is important for directing ω-ACTX-1 precursors to a specific secretory pathway in the venom gland. The mature toxin sequence is more variable, with substitutions observed at 16 out of 37 sites relative to ω-ACTX-Ar1a. Spiders are generalist predators, and these variations in the mature toxin sequence are presumed to provide the spider with a mini-combinatorial library of toxin isoforms for targeting variants of the target ion channel in a wide variety of arthropod prey [32].

Curiously, the propeptide sequence varies significantly between sexes. The three toxin variants isolated from the venom gland of the male *A. robustus* specimen all have identical 19-residue propeptide sequences. Surprisingly, however, the propeptide sequences in the two toxin variants isolated from the venom gland of the female *A. robustus* specimen have only limited homology with the male paralogs, although the Arg-Arg dipeptide sequence preceding the propeptide cleavage site is strictly conserved. The reason for these sex-related differences in the propeptide sequence, as well as the genetic mechanism underlying this sexual dichotomy, is unclear. Moreover, while most previously reported spider toxin propeptide sequences are highly acidic [12], the overall charge on the ω-ACTX-Ar1 propeptides ranges from −2 to +2.

3.5. Block of insect M-LVA and HVA Ca_v channels by ω-ACTX-Ar1a and ω-ACTX-Hv1a

To test the hypothesis that ω-ACTX-1 toxins block insect Ca_v channels, we investigated the effect of ω-ACTX-Ar1a and ω-ACTX-Hv1a on insect Ca_v channels in DUM neurons of the cockroach *P. americana*. To prevent Ca^{2+}-induced rundown of Ca^{2+} currents, Ba^{2+} was used as a charge carrier instead of Ca^{2+} [23]. Since Ba^{2+} currents (I_{Ba}) are larger than Ca^{2+} currents, the normal concentration was reduced to 3 mM to decrease the risk of voltage errors due to series resistance issues. The complete block of currents following the addition of 500 μM cadmium confirmed that the inward currents recorded were carried through Ca_v channels (data not shown).

Two subtypes of Ca_v channels have been described in cockroach DUM neurons: M-LVA and HVA Ca_v channels [23,33]. Unfortunately, despite differences in the kinetic and pharmacological properties of M-LVA and HVA Ca_v channels, there remains no mechanism for recording one current in isolation from the other as no peptide or organic blockers are available that exclusively block one type of current and not the other [23]. As previously described, depolarising pulses to different levels (−30 mV and +30 mV) were used to investigate the actions of the ω-ACTX-1 toxins on M-LVA and HVA Ca_v channels, respectively [23,33]. Macroscopic I_{Ba} through Ca_v channels were elicited by 100-ms depolarising command pulses from a V_h of −90 mV. Inward I_{Ba} were evoked by depolarising pulses to −30 mV (M-LVA Ca_v channel currents dominating) and +30 mV (HVA Ca_v channel currents dominating) [23]. Depolarisations to −30 mV (Fig. 4) caused a large inward current with slow decaying component, consistent with a reduction in Ca^{2+}-dependent fast inactivation due to the use of Ba^{2+} as the charge carrier [23], whereas depolarisations to +30 mV elicited a smaller current with a fast decaying component (Fig. 5). To confirm that a −30 mV pulse preferentially elicits M-LVA Ca_v channel currents

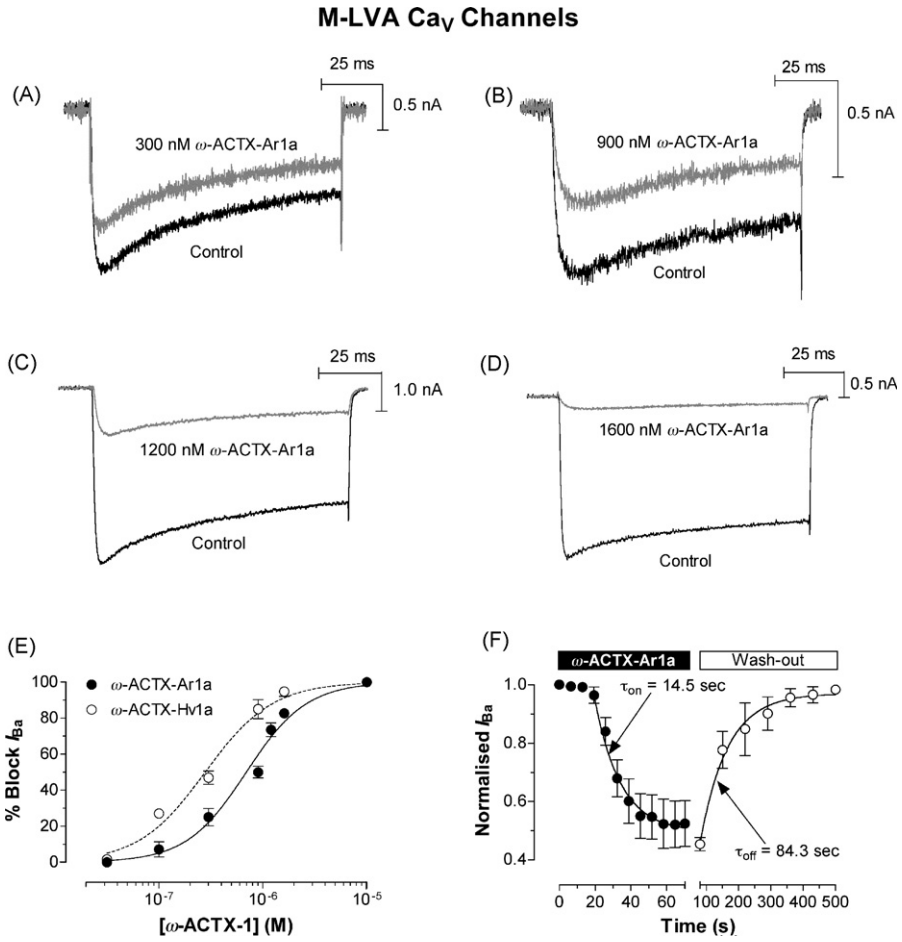

Fig. 4 – ω-ACTX-Ar1a blocks insect low-voltage-activated Ca_v channels. Low-voltage activated Ca_v channel currents in panels (A)–(D) were elicited by 100-ms depolarizing test pulses to −30 mV from a holding potential of −90 mV. Panels show typical concentration-dependent inhibition of M-LVA I_{Ba} following perfusion with 300 nM (A), 900 nM (B), 1200 nM (C) and 1600 nM (D) ω-ACTX-Ar1a. (E) Dose–response curve showing percentage block of M-LVA Ca_v channel currents by ω-ACTX-Ar1a (closed circles) and ω-ACTX-Hv1a (open circles) (n = 3–8). Data were fitted using Eq. (1). (F) On- and off-rates determined following application of 900 nM ω-ACTX-Hv1a and wash-out with toxin-free external solution (n = 5). Data were fitted using Eqs. (2) and (3).

we established that the insect M-LVA blocker ω-conotoxin MVIIC [23] produced selective inhibition of currents at −30 mV, rather than those elicited at +30 mV (HVA currents predominating). Application of 1 μM ω-conotoxin MVIIC caused a 48.4 ± 9.4% (n = 3) reduction in peak I_{Ba} in DUM neurons at a test pulse of −30 mV and only 18.4 ± 9.6% (n = 3) at a test pulse of +30 mV. This is similar to previously reported values [23].

Both ω-ACTX-Ar1a and ω-ACTX-Hv1a exerted a concentration-dependent tonic block of M-LVA Ca_v channels. Figs. 4 and 5 show the effects of increasing concentrations of ω-ACTX-Ar1a on peak I_{Ba} amplitude elicited by a 100-ms depolarizing test pulse to −30 or +30 mV from a holding potential of −90 mV every 10 s. The addition of 300 nM ω-ACTX-Ar1a resulted in a block of peak I_{Ba} of 25 ± 5% (n = 5) within 5 min at −30 mV (Fig. 4A), and 29 ± 3% (n = 3) block of depolarising pulses to +30 mV (Fig. 5A). At a concentration of 900 nM ω-ACTX-Ar1a, this block increased to 50 ± 3% (n = 5) and 54 ± 7% (n = 3) at −30 mV (Fig. 4B) and +30 mV (Fig. 5B), respectively. However, total block was only achieved at concentrations above 1.6 μM. Washing with toxin-free solution restored peak I_{Ba} within 5–7 min. The peak I_{Ba} in the presence of ω-ACTX-Ar1a was expressed as a percentage of the control peak I_{Na} and the depression of peak amplitude, after 10 min of perfusion, was plotted against toxin concentration. By fitting the concentration-response curve of the inhibition of peak I_{Ba} using a Logistic function (Eq. (1) in Section 2) the concentration at half-maximal block (IC_{50}) of M-LVA Ca_v channels was determined to be 692 nM for ω-ACTX-Ar1a and 279 nM for ω-ACTX-Hv1a (Fig. 4E). The IC_{50} values for block of HVA Ca_v channels were 644 nM for ω-ACTX-Ar1a and 1080 nM for ACTX-Hv1a (Fig. 5E). Despite a clear blocking action, both toxins failed to alter activation or inactivation kinetics, such that the time to peak current and the timecourse of current decay was not significantly affected at concentrations of ω-ACTX-Ar1a up to 1.6 μM. The time course of ω-ACTX-Ar1a association and dissociation were relatively slow and described by single exponential functions with a τ_{on} of 14.5 ± 1.7 s (n = 5) for M-LVA Ca_v channels (Fig. 4F) and 22.8 ± 5.8 (n = 5) for HVA

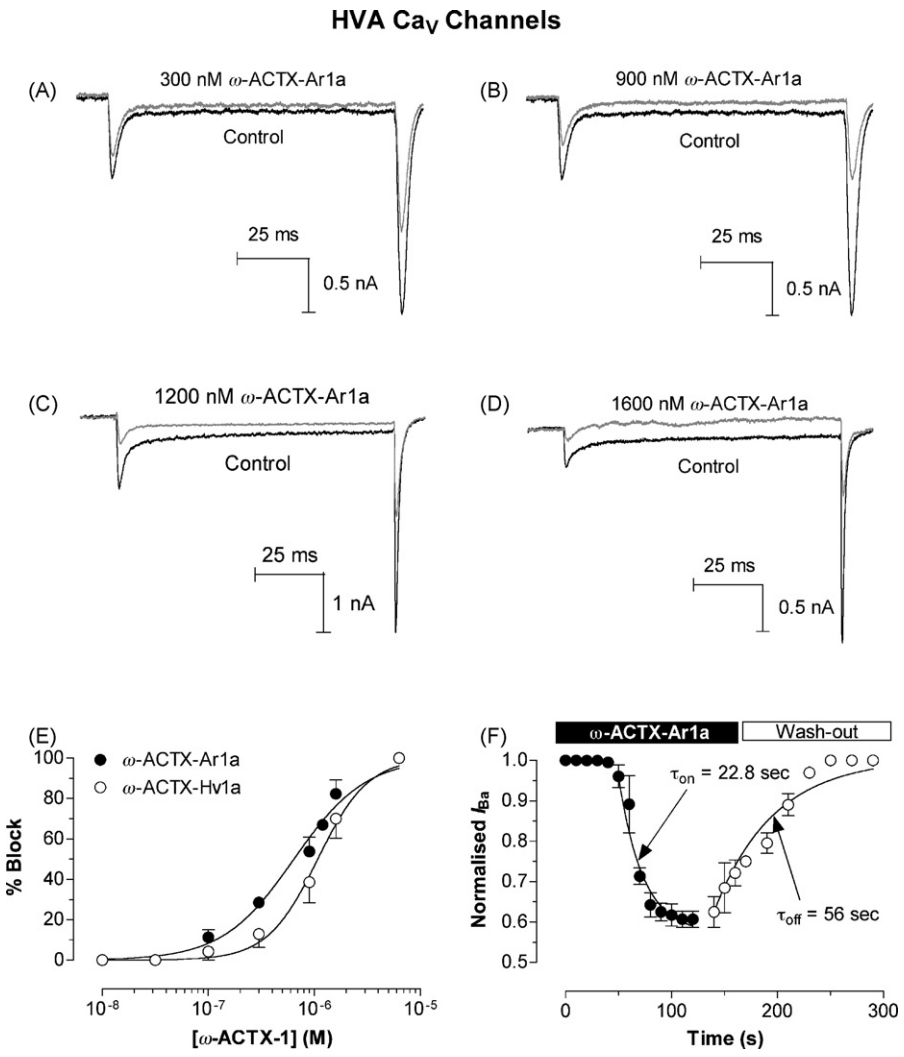

Fig. 5 – ω-ACTX-Ar1a blocks insect high-voltage activated Ca_v channels. High-voltage-activated Ca_v channel currents in panels (A)–(D) were elicited by 100 ms depolarizing test pulses to +20 mV from a holding potential of −90 mV. Panels show typical concentration-dependent inhibition of HVA I_{Ba} following perfusion with 300 nM (A), 900 nM (B) 1200 nM (C) and 1600 nM (D) ω-ACTX-Ar1a. (E) Dose–response curve showing percentage block of HVA Ca_v channel currents by ω-ACTX-Ar1a (closed circles) and ω-ACTX-Hv1a (open circles) (n = 3–5). Data were fitted using Eq. (1). (F) On- and off-rates determined following application of 900 nM ω-ACTX-Hv1a and washout with toxin-free external solution (n = 5). Data were fitted using Eqs. (2) and (3).

channels (Fig. 5F). The recovery after washout with toxin-free external solution was slow but complete with a τ_{off} of 84.3 ± 10.0 s (n = 5) for M-LVA Ca_v channels (Fig. 4F) and 56.0 ± 14.7 s (n = 5) for HVA channels (Fig. 5F). These slow on- and off-rates from DUM neuron Ca_v channels have been previously noted with peptide toxins such as ω-conotoxin GVIA and ω-conotoxin MVIIC [23] and CSTX-1 from *Cupiennius salei* venom [34].

3.6. *Effects on the voltage-dependence of M-LVA and HVA Ca_v channel activation*

To determine if the tonic block of Ca_v channels was due to a depolarising shift in the voltage-dependence of channel activation, we determined the action of ω-ACTX-Ar1a and ω-ACTX-Hv1a on current–voltage relationships. Families of I_{Ba} were generated by 100-ms test pulses from V_h (−90 mV) to a maximum of +30 mV in 10-mV increments, every 10 s. Typical effects of ω-ACTX-Ar1a on I_{Ba} were recorded before (Fig. 6Aa), and after (Fig. 6Ab) perfusion with 900 nM toxin. The I_{Ba}–V relationship was determined from the maximal I_{Ba} values at each potential (Fig. 6B). Data were normalised against peak maximal control I_{Ba} and fitted with Eq. (4) (see Section 2). Similar thresholds of activation in pre- and post-toxin conditions were observed for I_{Ba} and no significant shift was observed in the voltage at half-maximal activation, $V_{1/2}$, or slope factor, s. There was also little change (<3 mV) in the apparent reversal potential, V_{rev}, in post-toxin recordings, indicating that the ionic selectivity of Ca_v channels was not altered by ω-ACTX-Ar1a or ω-ACTX-Hv1a. In addition, at a concentration of 900 nM, both toxins produced a voltage-independent block at all test potentials (Fig. 6C).

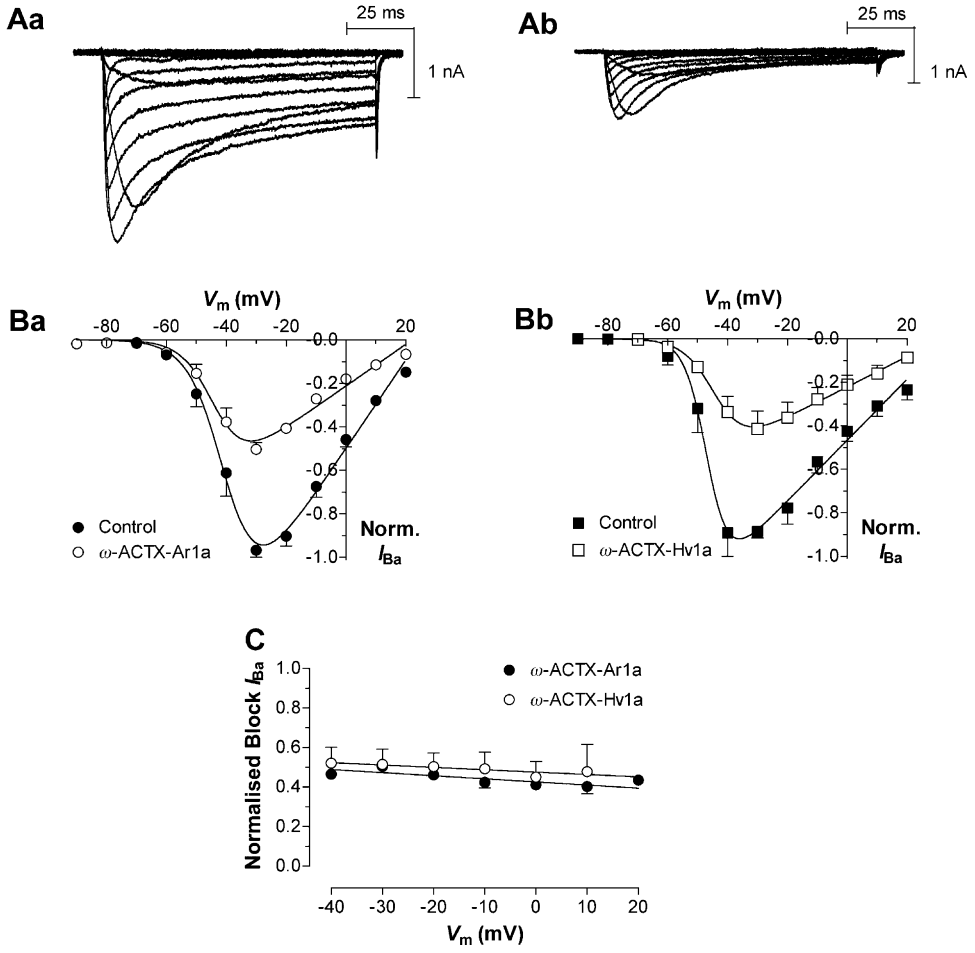

Fig. 6 – Voltage-dependence of Ca_v channel activation. Families of Ca_v channel currents were elicited by depolarizing test pulses to +30 mV from a holding potential of −90 mV in 10-mV steps. (A) Typical superimposed current traces recorded before (Aa) and after (Ab) a 10-min perfusion with 900 nM ω-ACTX-Ar1a. (B) Peak I_{Ba}/V relationship recorded before (closed symbols) and after (open symbols) application of 900 nM ω-ACTX-Ar1a (Ba, $n = 4$) and 900 nM ω-ACTX-Hv1a (Bb, $n = 4$). Data were fitted with Eq. (4). (C) Voltage-independent block of I_{Ba} by 900 nM ω-ACTX-Ar1a (closed circles, $n = 4$) and 900 nM ω-ACTX-Hv1a (open circles, $n = 4$). Data represent the normalized block at each test potential and were fitted by linear regression.

3.7. *Effects on Na_v and K_v channels*

To date, there are no reports in the literature investigating potential effects of any member of the ω-ACTX-1 family on insect ion channels except for the Ca_v channel. The relatively high IC_{50} values for both toxins on Ca_v channels suggested that they perhaps might target additional ion channels. It has been previously noted that peptide toxins can exert their actions both within and across voltage-gated ion channel families. This promiscuous activity has already been noted with other toxins targeting Ca_v channels such as SNX482, ω-agatoxin IVA, and protoxins I and II [35–38]. Accordingly, we examined the actions of ω-ACTX-Ar1a on both Na_v and K_v channel currents, present in cockroach DUM neurons. In contrast to the marked block of M-LVA and HVA I_{Ba}, no significant change was seen in global potassium channel current amplitude or time course, or the voltage-dependence of potassium channel activation, following perfusion of 1 μM ω-ACTX-Ar1a for up to 10 min (Fig. 7Ab–Eb). When tested on Na_v channels, 1 μM ω-ACTX-Ar1a caused a modest 18 ± 5% ($n = 4$) block of peak I_{Na} at test pulses to −10 mV, with no effect on activation or inactivation kinetics or the voltage-dependence of Na_v channel activation (Fig. 7Aa–Ea). It is clear, therefore, that ω-ACTX-Ar1a and ω-ACTX-Hv1a selectively block Ca_v channel currents in the insect CNS although at higher concentrations they may have non-selective effects on other voltage-gated ion channels, particularly Na_v channels.

4. Discussion

The initial aim of the present project was to determine whether it was possible to isolate insect-selective neurotoxins from the venom of the Sydney funnel-web spider, *A. robustus*. However, the identification a 37-residue *A. robustus* peptide toxin with high sequence homology to members of the ω-ACTX-1 family of toxins, including complete conservation of the cysteine and insectophore residues, led us to more

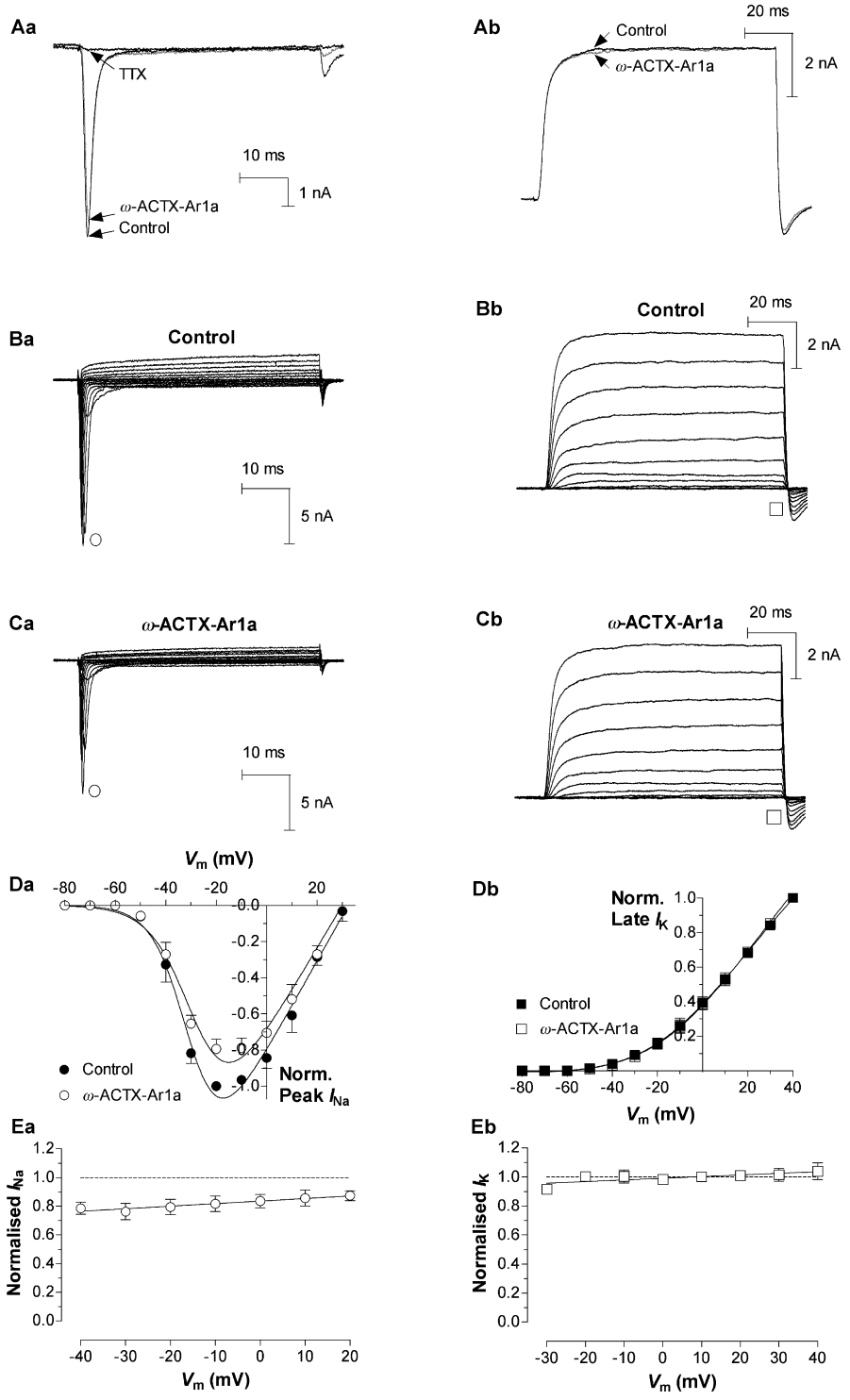

Fig. 7 – Effects of ω-ACTX-Ar1a on insect Na_v and K_v channels. Typical whole-cell macroscopic I_{Na} (left hand panels) and I_K (right hand panels) recorded from cockroach DUM neurons. Macroscopic currents in panel Aa were elicited by 100-ms depolarizing test pulses to −10 mV from a holding potential of −80 mV. (Aa) Partial inhibition of peak of I_{Na} following a 10 min perfusion with 1 μM ω-ACTX-Ar1a. The current was completely blocked by 100 nM TTX indicating that this current was mediated exclusively, via Na_v channels. (Ab) Representative traces illustrating the lack of inhibition of global K_v channel currents by 1 μM ω-ACTX-Ar1a. (B–C) Typical families of Na_v (Ba, Ca) and K_v (Bb, Cb) channel currents elicited by depolarizing test pulses to +70 and +40 mV, respectively, from a holding potential of −90 mV in 10-mV steps. Data shown represents superimposed current traces recorded before (B) and after (C) a 10-min perfusion with 1 μM ω-ACTX-Ar1a. (D) Peak I_{Na}/V (Da, $n = 4$) and late I_K/V (Db, $n = 3$) relationships recorded before (closed circles), and after (open circles), application of 1 μM ω-ACTX-Ar1a. (E) Voltage-independent block of I_{Na} (Ea, $n = 4$) and I_K (Eb, $n = 3$) by 900 nM ω-ACTX-Ar1a. Data represent the normalized block at each test potential and were fitted by linear regression. The dashed lines represent 0% block.

thoroughly characterize the effects of these toxins on insect Ca_v channels. Given that the newly isolated peptide toxin also blocks insect Ca_v channels we have named it ω-ACTX-Ar1a, in accordance with the established nomenclature system used for naming funnel-web spider toxins [10] and conotoxins [39].

Acute toxicity tests in house crickets revealed that ω-ACTX-Ar1a induces an initial excitatory response followed by a depressant phenotype prior to death. This biphasic phenotype has previously been described following injection of members of the ω-ACTX-1 family into a wide range of insects, including coleopterans, orthopterans, lepidopterans and dipterans [9,10,16,17] and has been noted in recordings of compound action potentials induced by ω-ACTX-Hv1a in a *Drosophila* CNS preparation [40]. ω-ACTX-Ar1a is a moderately potent neurotoxin when compared to other members of the ω-ACTX-Hv1 family, which have effective doses ranging from 84–1384 pmol/g in house crickets [9]. ω-ACTX-Hv1b, its closest homolog by amino acid sequence, has an LD_{50} of 224 ± 7 pmol/g [9] which is almost identical to the LD_{50} of 236 ± 28 pmol/g obtained for ω-ACTX-Ar1a. Although ω-ACTX-Ar1a is three-fold less potent than ω-ACTX-Hv1a, it should be noted the ω-ACTX-Hv1 family is one of the most potent insecticidal neurotoxin families discovered to date. Other insect-selective neurotoxins, such as those from the spider *Tegenaria agrestis*, and the primitive weaving spider *Diguetia canities*, have median effective doses ranging from 0.89 to 2.6 nmol/g and 0.38–3.2 nmol/g, respectively [41,42].

Although the insectophore of ω-ACTX-Ar1a was not determined experimentally, the major (Pro^{10}, Asn^{27}, and Arg^{35}) and minor (Gln^{9}, Tyr^{13}) insectophore residues of ω-ACTX-Hv1a [9,11] are strictly conserved. The high homology (86%) in primary structure with ω-ACTX-Hv1a, including the same number and spacing of cysteine residues, strongly suggests that ω-ACTX-Ar1a also contains three disulfide bonds that form the same ICK structural motif that is a prominent feature of this family of toxins [43], and almost certainly has a solution structure similar to ω-ACTX-Hv1a. Accordingly the structure of ω-ACTX-Ar1a was modeled on ω-ACTX-Hv1a (PDB code 1AXH) using the automated protein homology-modelling server SWISS-MODEL [44,45] (Fig. 1C). This revealed that, apart from residues 2–3, the amino acids that differ in ω-ACTX-Ar1a are located, relative to the face of the toxin containing the insectophore residues, primarily on the side and rear faces of the toxin. Thus, these sequence variations are unlikely to affect the disposition of either the major or minor insectophore.

Nevertheless, the present study identified a three-fold loss in lethality in comparison to ω-ACTX-Hv1a using the cricket bioassay (ω-ACTX-Ar1a LD_{50} 236 ± 28 pmol/g versus ω-ACTX-Hv1a LD_{50} 84 ± 10 pmol/g at 48 h [9]). Despite a structurally disordered N-terminus, the first three amino acid residues of ω-ACTX-Hv1a have been shown to be important for toxicity, as indicated by a slight reduction in insecticidal potency when these three residues are deleted [9]. Thus, the variations at position 2 and 3 in ω-ACTX-Ar1a may account for the lower toxicity in crickets compared with ω-ACTX-Hv1a. However, the decrease in potency is more likely due to substitution of Asn^{16} by a His residue, since Asn^{16} in ω-ACTX-Hv1a forms part of an additional minor pharmacophore in crickets, but not flies or cockroaches [12].

The IC_{50} values for the block of M-LVA and HVA Ca_v channels by ω-ACTX-Ar1a and ω-ACTX-Hv1a are not significantly different from that reported for block of macroscopic I_{Ba} by ω-ACTX-Hv1a in unidentified cockroach neurons [10]. Importantly, the three-fold lower toxicity of ω-ACTX-Ar1a following injection into house crickets, parallels the three-fold reduction in IC_{50} values for block of M-LVA Ca_v channels. This suggests that the slightly lower toxicity of ω-ACTX-Ar1a may be due to differences between ω-ACTX-1 toxins in their interaction with the Ca_v channel target in crickets rather than pharmacokinetic issues related to bioavailability of the toxins at the target site. In addition, actions on DUM neurons may suggest a CNS target for ω-ACTX-1 toxins. This is supported by the finding that ω-ACTX-Hv1a crossed the blood-brain barrier and depressed activity in *P. americana* and *Drosophila melanogaster* CNS preparations at low nanomolar doses, whereas it had no effect on peripheral neuromuscular synapses [17].

Previous studies using cockroach DUM neurons have identified the presence of both M-LVA and HVA Ca_v channel subtypes in cockroach DUM neurons [22,33]. Interestingly, these are distinct from the LVA (T-type) and HVA (P/Q-, N-, L- and R-type) Ca_v channels described in vertebrates, since the pharmacological and electrophysiological distinctions used for vertebrate Ca_v channels are not applicable to invertebrates [22,23,33,46–50]. This difference no doubt underlies the phyletic specificity of the ω-ACTX-1 family. Importantly, ω-ACTX-Hv1a has been shown to have no effect on whole-cell Ca_v channel currents in a variety of vertebrate neuron preparations at concentrations as high as 1 μM [10], and it does not block cloned rat $Ca_v2.1$ (P/Q-type), $Ca_v2.2$ (N-type), or $Ca_v1.2$ (L-type) Ca_v channels at concentrations as high as 10 μM [12].

Unfortunately, while organic compounds such as verapamil, SKF93635, ω-conotoxin GVIA and ω-conotoxin MVIIC have been useful in identifying the existence of HVA and M-LVA currents in DUM neurons [23,33], the differential sensitivity of Ca_v channel subtypes to these blockers is inadequate to completely separate these currents by pharmacological means [46]. Thus it is not possible, at present, to definitively identify the Ca_v channel subtype targeted by ω-ACTX-1 toxins in insects. Nevertheless, the voltage-independent block of currents at depolarizing test pulses to −30 mV (M-LVA Ca^{2+} currents dominating) would strongly suggest that ω-ACTX-Ar1a blocks insect M-LVA Ca_v channels. The similar degree of block at +30 mV (HVA Ca^{2+} currents dominating) indicates that ω-ACTX-1 toxins also block insect HVA currents. Thus the molecular epitope recognized by ω-ACTX-1 toxins maybe common to both M-LVA and HVA Ca_v channels, and this epitope is most likely located in the pore region of the channel given that these toxins do not modify gating.

We were unable to determine whether DUM neuron T-type-like LVA calcium channels [22] are sensitive to ω-ACTX-1 toxins since, as reported in the study of Wicher and Penzlin [23], we did not observe such currents (activating at voltages negative to −50 mV) in our preparations. It is also highly unlikely that the effects of the ω-ACTX-1 toxins seen in the present study can be explained by an inhibition of the maintained LVA non-selective calcium/sodium current [51] as this current has a threshold of −65 mV, and was not observed in any of our recordings. This is most likely because

of the presence of 2–3 mM ATP and 0.5 μM TTX which would almost abolish this current.

The selectivity of the ω-ACTX-1 toxins for insect versus vertebrate Ca_v channels no doubt arises from the significant pharmacological and kinetic differences between the two phyla. First, the electrophysiological differences between insect M-LVA and HVA Ca_v channels appear to be less prominent than in vertebrates. For example, the voltage range of activation of M-LVA and HVA Ca_v channels in insect neurons does not differ to the extent observed for these two channel superfamilies in vertebrates. In insects, the presence of both M-LVA and HVA Ca_v channel currents can only be demonstrated pharmacologically, because the currents evoked at negative potentials have a different toxicological profile than the currents that require more depolarized potentials for activation [23]. Moreover, inactivation of vertebrate L-type HVA currents can be reduced by replacing Ca^{2+} with Ba^{2+} as the charge carrier, which indicates that Ca^{2+}-dependent mechanisms play a crucial role in channel inactivation. LVA currents in vertebrate neurons are transient with Ba^{2+} as the charge carrier, suggesting that T-type channels inactivate in a Ca^{2+}-independent manner. In contrast, the transient nature of M-LVA currents in cockroach DUM neurons is similar to vertebrate L-type HVA currents, predominantly caused by Ca^{2+}-dependent inactivation, and is thus abolished if Ba^{2+} is used as the charge carrier [23]. In addition, vertebrate T-type channel antagonists such as amiloride are ineffective on insect M-LVA Ca_v channels [23]. Furthermore, both M-LVA and HVA Ca^{2+} currents in cockroach neurons can be inhibited by peptide toxins (ω-conotoxin MVIIC and ω-conotoxin GVIA, respectively) that act selectively on only HVA Ca_v channel types in vertebrate neurons [23]. Importantly, inhibition by these toxins often occurs with much slower kinetics than in vertebrate preparations ([23] and the present study). These observations indicate that Ca_v channels in cockroach neurons are functionally very different to vertebrate HVA Ca_v channels, despite ~65% identity in their amino acid sequences [46]. Finally HVA Ca_v channel currents of DUM neurons were reported to show sensitivity to both phenylalkylamines and benzylalkylamines but, unlike vertebrates, not dihydropyridines such as nifedipine [23]. Given these significant differences in insect and vertebrate Ca_v channels it is perhaps not surprising that ω-ACTX-1 toxins are able to selectively target invertebrate Ca_v channels.

Previous studies have reported a biphasic action of ω-ACTX-Hv1a in *Drosophila* CNS compound action potentials with initial neuroexcitation followed by inhibition at higher concentrations [17]. The neuroexcitation correlates with the early spastic paralysis phase observed in housefly larvae treated with ω-ACTX-Hv1a [17] and the effects of ω-ACTX-Ar1a in house crickets seen in the present study. One possible mechanism suggested by Bloomquist [17] was that multiple subtypes of CNS Ca_v channels could be involved, one responsible for excitation and the other for inhibition of neurotransmission. There could be preferential sensitivity of Ca_v channels in an inhibitory pathway participating in the patterned CNS discharge. Since there is no evidence that ω-ACTX-1 toxins cause any hyperpolarizing shift in the voltage-dependence of Ca_v channel activation, attenuation of an inhibitory influence could result in CNS disinhibition with ensuing neuroexcitation. Alternatively, it is known that Ca_v channels subtypes in insect neurons mediate different actions on transmitter release. In spontaneously active cockroach DUM neurons, it has been demonstrated that LVA Ca_v channels contribute to the predepolarizing phase of action potentials [22,49]. Therefore block of LVA Ca_v channels leads to slower predepolarization resulting in a slower spontaneous action potential firing frequency and a consequent decrease in transmitter release. Although the functional significance of HVA Ca_v channels in cockroach DUM neurons has not been directly assessed, it has been postulated that these channels play a key role in the control of the action potential hyperpolarization, via the modulation of the large conductance calcium-activated potassium channels (BK_{Ca}) encoded by the slowpoke (Slo) gene [27]. The BK_{Ca} current contributes to membrane repolarization in *Drosophila* nerve terminals and helps to limit transmitter release by narrowing presynaptic action potentials, and reducing depolarization, to decrease Ca^{2+} entry into the nerve terminal [52]. This action is also seen at vertebrate central and peripheral nerve terminals [53–55]. Therefore block of HVA Ca_v channels leads to inhibition of BK_{Ca} channels resulting in an increase in action potential duration and a decrease in the fast afterhyperpolarization [56,57]. Block of HVA Ca_v channels by ω-ACTX-1 toxins most likely results in an increase in transmitter release. Thus the actions of ω-ACTX-1 toxins to block both M-LVA and HVA Ca_v channels could explain the biphasic effects seen in the acute toxicity tests and in electrophysiological recordings from *Drosophila* CNS preparations [17] rather than selective block of inhibitory pathways leading to disinhibition.

Notwithstanding these actions, it has been previously noted that spider peptide neurotoxins can exert their actions both within, and across, voltage-gated ion channel families. For example SNX482 is a known blocker of R-type [58] and P/Q-type [35] Ca_v channels. This toxin has also been shown to delay Na_v channel inactivation and partially block I_{Na} in bovine chromaffin cells at similar concentrations to those that block I_{Ca} [35]. This dual activity on Na_v and Ca_v channels has been reported for Protoxin-I and -II (ProTx-I and -II) that act as gating modifiers to inhibit $Na_v1.2$, 1.5, 1.7 and 1.8 channels by causing a depolarizing shift in the voltage-dependence of activation [37]. However ProTx-1 also potently blocks $Ca_v3.1$ (T-type) channels and partially inhibits $K_v1.3$ and $K_v2.1$ channels [37] while ProTX-II blocks $Ca_v3.x$ (T-type) and $Ca_v1.x$ (L-type) channels [38]. Most relevant to the present study on insect neurons is the P/Q-type Ca_v channel blocker ω-agatoxin IVA which also decreased TTX-sensitive I_{Na} amplitude, enhanced I_{Na} decay, and led to a slower recovery from Na_v channel inactivation in cockroach DUM neurons [36]. Therefore, the minor block of Na_v channels by ω-ACTX-Ar1a is not without precedence.

It may be argued that the IC_{50} values of the ω-ACTX-1 toxins are rather high and that the toxins may actually target other channels or receptors to produce toxicity. However, other well-characterized peptide toxins that block Ca_v channels, such as ω-conotoxin GVIA and ω-conotoxin MVIIC, also have high IC_{50} values on insect neurons in comparison to activities on vertebrate channels [23]. Moreover, it should be noted that insects have a much smaller repertoire of Ca_v channel subtypes than vertebrates [46]. *D. melanogaster*, for example,

harbours only a single ortholog of each of the vertebrate Ca_v1, Ca_v2, and Ca_v3 subtypes. Thus, unlike vertebrates, which can survive a knockout of some Ca_v channel subtypes, Ca_v channel knockouts in insects are invariably lethal [46]. Thus, it is perhaps not surprising that even moderate inhibition of insect Ca_v channels can have profound neurotoxic effects. Although the ω-ACTX-1 toxins block two types of insect Ca_v channels with only moderate potency and induce an even weaker block of insect Na_v channels, the combined actions on these three channels would be expected to markedly affect the CNS of insects. The excitatory phenotype observed after injection of ω-ACTX-Ar1a may result from a block of HVA Ca_v channels while the subsequent depressant phenotype could arise from the combined block of M-LVA Ca_v channels and modest block of Na_v channels.

The high phylogenetic specificity of these toxins recommends them as lead compounds for the development of new insecticides with novel modes of action [30]. This may include the development of small mimetics that could be used as foliar sprays, orally active acaricidal and insecticidal agents, and recombinant baculoviruses and transgenic crops containing ω-ACTX-1 transgenes [59]. Most importantly, however, these toxins validate insect Ca_v channels as a novel insecticide target, and they may prove to be useful ligands for medium- to high-throughput assays in insecticide discovery programs [46].

Acknowledgements

The authors would like to thank Roger Drinkwater of Xenome Ltd. for help with preparation of cDNA libraries. This work was supported by an ARC Discovery grant DP0559396 to GMN, PH, KWB, WCH and GFK, and NSF grant MCB0234638 to GFK.

REFERENCES

[1] World Health Organisation. Vector resistance to insecticides. 15th Report of the WHO Expert Committee on Vector Biology and Control. World Health Org Tech Rep Ser 1992;818:1–62.
[2] Georghiou GP. Overview of insecticide resistance. ACS Symp Ser 1990;421:18–41.
[3] Oerke E-C, Dehne H-W. Safeguarding production-losses in major crops and the role of crop protection. Crop Protect 2004;23:275–85.
[4] Gubler DJ. Resurgent vector-borne diseases as a global health problem. Emerg Infect Dis 1998;4:442–50.
[5] Bravo A, Gill SS, Soberón M. *Bacillus thuringiensis* mechanisms and use. In: Gilbert LI, Iatrou K, Gill SS, editors. Comprehensive molecular insect science. Elsevier; 2005. p. 175–206.
[6] Cory JS, Hirst ML, Williams T, Hails RS, Goulson D, Green BM, et al. Field trial of a genetically improved baculovirus insecticide. Nature 1994;370:138–40.
[7] Khan SA, Zafar Y, Briddon RW, Malik KA, Mukhtar Z. Spider venom toxin protects plants from insect attack. Transgenic Res 2006;15:349–57.
[8] Mukherjee AK, Sollod BL, Wikel SK, King GF. Orally active acaricidal peptide toxins from spider venom. Toxicon 2006;47:182–7.
[9] Wang X-H, Smith R, Fletcher JI, Wilson H, Wood CJ, Howden ME, et al. Structure-function studies of ω-atracotoxin, a potent antagonist of insect voltage-gated calcium channels. Eur J Biochem 1999;264:488–94.
[10] Fletcher JI, Smith R, O'Donoghue SI, Nilges M, Connor M, Howden ME, et al. The structure of a novel insecticidal neurotoxin, ω-atracotoxin-HV1, from the venom of an Australian funnel web spider. Nat Struct Biol 1997;4:559–66.
[11] Tedford HW, Fletcher JI, King GF. Functional significance of the β hairpin in the insecticidal neurotoxin ω-atracotoxin-Hv1a. J Biol Chem 2001;276:26568–76.
[12] Tedford HW, Gilles N, Ménez A, Doering CJ, Zamponi GW, King GF. Scanning mutagenesis of ω-atracotoxin-Hv1a reveals a spatially restricted epitope that confers selective activity against insect calcium channels. J Biol Chem 2004;279:44133–40.
[13] Pallaghy PK, Neilsen KJ, Craik DJ, Norton RS. A common structural motif incorporating a cystine knot and a triple-stranded β-sheet in toxic and inhibitory polypeptides. Protein Sci 1994;3:1833–9.
[14] Pallaghy PK, Norton RS. Refined solution structure of ω-conotoxin GVIA: implications for calcium channel binding. J Pept Res 1999;53:343–51.
[15] Craik DJ, Daly NL, Waine C. The cystine knot motif in toxins and implications for drug design. Toxicon 2001;39:43–60.
[16] Atkinson RK, Tyler MI, Vonarx EJ, Howden MEH. Insecticidal toxins derived from funnel web (*Atrax* or *Hadronyche*) spiders. International Patent WO 93/15108; 1993, August 5.
[17] Bloomquist JR. Mode of action of atracotoxin at central and peripheral synapses of insects. Invert Neurosci 2003;5:45–50.
[18] Vonarx EJ, Tyler MI, Atkinson RK, Howden MEH. Characterization of insecticidal peptides from venom of Australian funnel-web spiders. J Venom Anim Toxins 2006;12:215–33.
[19] Ginsborg BL, Warriner J. The isolated chick biventer cervicis nerve-muscle preparation. Br J Pharmacol 1960;15:410–1.
[20] Frohman MA. Rapid amplification of complementary DNA ends for generation of full-length complementary DNAs: thermal RACE. Meth Enzymol 1993;218:340–56.
[21] Frohman MA, Dush MK, Martin GR. Rapid production of full-length cDNAs from rare transcripts: amplification using a single gene-specific oligonucleotide primer. Proc Natl Acad Sci USA 1988;85:8998–9002.
[22] Grolleau F, Lapied B. Two distinct low-voltage-activated Ca^{2+} currents contribute to the pacemaker mechanism in cockroach dorsal unpaired median neurons. J Neurophysiol 1996;76:963–76.
[23] Wicher D, Penzlin H. Ca^{2+} currents in central insect neurons: electrophysiological and pharmacological properties. J Neurophysiol 1997;77:186–99.
[24] Sinakevitch IG, Geffard M, Pelhate M, Lapied B. Anatomy and targets of dorsal unpaired median neurones in the terminal abdominal ganglion of the male cockroach *Periplaneta americana* L. J Comp Neurol 1996;367:147–63.
[25] Barry PH. JPCalc, a software package for calculating liquid junction potential corrections in patch-clamp, intracellular, epithelial and bilayer measurements and for correcting junction potential measurements. J Neurosci Meth 1994;51:107–16.
[26] Bezanilla F, Armstrong CM. Inactivation of sodium channels. I. Sodium current experiments. J Gen Physiol 1977;70:594–666.
[27] Lapied B, Malécot CO, Pelhate M. Ionic species involved in the electrical activity of single adult aminergic neurones isolated from the sixth abdominal ganglion of the cockroach *Periplaneta americana*. J Exp Biol 1989;144:545–9.

[28] Atkinson RK, Vonarx EJ, Howden MEH. Effects of whole venom and venom fractions from several Australian spiders, including *Atrax* (*Hadronyche*) species, when injected into insects. Comp Biochem Physiol 1996;114C:113–7.
[29] Bendtsen JD, Nielsen H, von Heijne G, Brunak S. Improved prediction of signal peptides: SignalP 3.0. J Mol Biol 2004;340:783–95.
[30] Tedford HW, Sollod BL, Maggio F, King GF. Australian funnel-web spiders: master insecticide chemists. Toxicon 2004;43:601–18.
[31] Wang X-H, Connor M, Wilson D, Wilson H, Nicholson GM, Smith R, et al. Biopesticide panning: discovery of a potent and highly specific peptide antagonist of insect calcium channels. J Biol Chem 2001;276:40306–12.
[32] Sollod BL, Wilson D, Zhaxybayeva O, Gogarten JP, Drinkwater R, King GF. Were arachnids the first to use combinatorial peptide libraries? Peptides 2005;26:131–9.
[33] Wicher D, Penzlin H. Ca^{2+} currents in cockroach neurones: properties and modulation by neurohormone D. Neuroreport 1994;5:1023–6.
[34] Kubista H, Mafra RA, Chong Y, Nicholson GM, Beirao PS, Cruz JS, et al. CSTX-1, a toxin from the venom of the hunting spider *Cupiennius salei*, is a selective blocker of L-type calcium channels in mammalian neurons. Neuropharmacology 2007;51:1650–62.
[35] Arroyo G, Aldea M, Fuentealba J, Albillos A, Garcia AG. SNX482 selectively blocks P/Q Ca^{2+} channels and delays the inactivation of Na^+ channels of chromaffin cells. Eur J Pharmacol 2003;475:11–8.
[36] Wicher D, Penzlin H. ω-Toxins affect Na^+ currents in neurosecretory insect neurons. Receptors Channels 1998;5:355–66.
[37] Middleton RE, Warren VA, Kraus RL, Hwang JC, Liu CJ, Dai G, et al. Two tarantula peptides inhibit activation of multiple sodium channels. Biochemistry 2002;41:14734–47.
[38] Kraus RL, Warren VA, Smith MM, Middleton RE, Cohen CJ. Modulation of $alpha_{1G}$ and $alpha_{1C}$ Ca channels by the spider toxin ProTx-II. Soc Neurosci Abstr 2000;623.
[39] Olivera BM, Miljanich GP, Ramachandran J, Adams ME. Calcium channel diversity and neurotransmitter release: the ω-conotoxins and ω-agatoxins. Annu Rev Biochem 1994;63:823–67.
[40] Bloomquist JR. Toxicology, mode of action and target site-mediated resistance to insecticides acting on chloride channels. Comp Biochem Physiol C 1993;106:301–14.
[41] Johnson JH, Bloomquist JR, Krapcho KJ, Kral Jr RM, Trovato R, Eppler KG, et al. Novel insecticidal peptides from *Tegenaria agrestis* spider venom may have a direct effect on the insect central nervous system. Arch Insect Biochem Physiol 1998;38:19–31.
[42] Krapcho KJ, Kral Jr RM, Vanwagenen BC, Eppler KG, Morgan TK. Characterization and cloning of insecticidal peptides from the primitive weaving spider *Diguetia canities*. Insect Biochem Mol Biol 1995;25:991–1000.
[43] King GF, Tedford HW, Maggio F. Structure and function of insecticidal neurotoxins from Australian funnel-web spiders. J Toxicol-Toxin Rev 2002;21:359–89.
[44] Schwede T, Kopp J, Guex N, Peitsch MC. SWISS-MODEL: an automated protein homology-modeling server. Nucl Acids Res 2003;31:3381–5.
[45] Guex N, Peitsch MC. SWISS-MODEL and the Swiss-PdbViewer: an environment for comparative protein modeling. Electrophoresis 1997;18:2714–23.
[46] King GF. Modulation of insect Ca_v channels by peptidic spider toxins. Toxicon 2007;49:513–30.
[47] Grolleau F, Lapied B. Separation and identification of multiple potassium currents regulating the pacemaker activity of insect neurosecretory cells (DUM neurons). J Neurophysiol 1995;73:160–71.
[48] Jeziorski MC, Greenberg RM, Anderson PA. The molecular biology of invertebrate voltage-gated Ca^{2+} channels. J Exp Biol 2000;203:841–56.
[49] Grolleau F, Lapied B. Dorsal unpaired median neurones in the insect central nervous system: towards a better understanding of the ionic mechanisms underlying spontaneous electrical activity. J Exp Biol 2000;203:1633–48.
[50] Wicher D. Peptidergic modulation of insect voltage-gated Ca^{2+} currents: role of resting Ca^{2+} current and protein kinases A and C. J Neurophysiol 2001;86:2353–62.
[51] Defaix A, Lapied B. Role of a novel maintained low-voltage-activated inward current permeable to sodium and calcium in pacemaking of insect neurosecretory neurons. Invert Neurosci 2005;5:135–46.
[52] Gho M, Ganetzky B. Analysis of repolarization of presynaptic motor terminals in *Drosophila* larvae using potassium-channel-blocking drugs and mutations. J Exp Biol 1992;170:93–111.
[53] Robitaille R, Charlton MP. Presynaptic calcium signals and transmitter release are modulated by calcium-activated potassium channels. J Neurosci 1992;12:297–305.
[54] Robitaille R, Garcia ML, Kaczorowski GJ, Charlton MP. Functional colocalization of calcium and calcium-gated potassium channels in control of transmitter release. Neuron 1993;11:645–55.
[55] Raffaelli G, Saviane C, Mohajerani MH, Pedarzani P, Cherubini E. BK potassium channels control transmitter release at CA3-CA3 synapses in the rat hippocampus. J Physiol (Lond) 2004;557:147–57.
[56] Wicher D, Berlau J, Walther C, Borst A. Peptidergic counter-regulation of Ca^{2+}- and Na^+-dependent K^+ currents modulates the shape of action potentials in neurosecretory insect neurons. J Neurophysiol 2006;95:311–22.
[57] Derst C, Messutat S, Walther C, Eckert M, Heinemann SH, Wicher D. The large conductance Ca^{2+}-activated potassium channel (pSlo) of the cockroach *Periplaneta americana*: structure, localization in neurons and electrophysiology. Eur J Neurosci 2003;17:1197–212.
[58] Newcomb R, Szoke B, Palma A, Wang G, Chen X, Hopkins W, et al. Selective peptide antagonist of the class E calcium channel from the venom of the tarantula *Hysterocrates gigas*. Biochemistry 1998;37:15353–62.
[59] Nicholson GM. Fighting the global pest problem: preface to the special Toxicon issue on insecticidal toxins and their potential for insect pest control. Toxicon 2007;49:413–22.